Nanoindentation of graphene-reinforced polypropylene nanocomposites laminated with carbon fibres

P. Enrique-Jimenez[1], S. Quiles-Díaz[2], H.J. Salavagione[2], M.A. Gómez-Fatou[2], F. Ania[1] and A. Flores[1]

[1]Instituto de Estructura de la Materia (IEM-CSIC), Serrano 119, 28006 Madrid, Spain
Email: patricia.enrique@csic.es
[2]Instituto de Ciencia y Tecnología de Polímeros (ICTP-CSIC), Juan de la Cierva 3, 28006, Madrid, Spain

Keywords: Nanoindentation, graphene, polypropylene nanocomposite, laminate, carbon fibre mats

Abstract

The mechanical properties of graphene-reinforced polypropylene nanocomposites laminated with alternating carbon fibre mats have been studied at a local scale by nanoindentation and results are correlated with morphological studies by means of scanning electron microscopy (SEM). Mechanical maps (storage modulus and hardness) have been obtained using indentation depths of a few tens of nanometres. Analysis of the distribution of $E´$ values close to and far away from isolated carbon fibres offers a comprehensive understanding of the role of graphene on the mechanical properties of the transition region between the reinforced matrix and the microsized fibres.

1. Introduction

Multilaminar systems alternating a graphene-reinforced commodity polymer and carbon fibre (CF) fabric are most attractive as multifunctional lightweight materials with important projections in the transportation industry. On the one hand, graphene can provide electrical conductivity, improved thermal stability and enhanced mechanical properties to the host matrix [1]. On the other hand, reinforcement also takes place at the microscale with the use of carbon fibres, leading to hierarchical materials.

Graphene distribution and interaction with the host matrix influences the nanoscale reinforcement while the interface between the reinforced polymer and the CF mats is crucial for the transverse properties and seems most relevant for the final material performance [2]. The occurrence of an interphase region that can provide a good transference of stresses between layers appears as a sound strategy to minimize the laminate failure. Previous studies on analogous multilaminar systems have shown that the presence of a carbonaceous filler in the polymer layer can improve the local mechanical properties of the interphase [2].

In this context, nanoindentation is here proposed as a convenient and versatile technique to measure the local mechanical properties of multilaminar hierarchically reinforced composites [3]. It only requires a small sample amount and is capable of yielding information on the mechanical behavior associated to very different scales: from several microns (related to the bulk performance of the material) to few tens of nanometers (related to the local properties).

In an earlier study, graphene was modified with low molecular weight PP brushes and incorporated in small amounts (≤ 2 vol.%) to the iPP host matrix [6]. It was found that Young's modulus increased up

to ≈ 100%. The present work approaches the study of the local mechanical properties of hierarchical composites based on graphene-reinforced isotactic polypropylene (iPP) and CF mats. Advanced nanoindentation techniques have been employed for this purpose. A discussion on the correlation between the local mechanical properties and the morphology of the laminates with modified and non-modified graphene is also offered.

2. Materials and methods

2.1. Materials

Isotactic polypropylene (iPP) was supplied by Repsol, Spain, with 95% isotacticity, $M_v = 179,000$ g/mol and polydispersity of 4.77. Graphene (G) was purchased from Avanzare Nanotechnology and it consists of 1 or 2 layers with lateral dimensions of 22 ± 5 μm and 9 ± 2 μm. The graphene surface was covalently modified to attach low molecular weight polypropylene chains in order to improve the dispersion of the nanofiller in the polymer matrix. The mixture of this modified graphene and polypropylene was named G-PP/iPP (1.9 vol.% graphene). For the sake of comparison, non-modified graphene was also mixed with iPP, giving rise to G/iPP (1.6 vol.% graphene). A full description of the modification procedure and material characterization is available in [6].

Polymer films of 0.2 mm thickness were obtained by hot compression molding. Afterwards, 3 films of iPP/graphene alternated with 2 mats of CF were hot pressed to prepare the laminates. Fig.1 shows a schematic example of a laminate. The final thickness of the laminates was around 0.9 mm and the fraction of CF was around 50 wt.%. Three laminates were prepared using one of the following polymer-based layers: neat PP (laminate denoted iPP+CF), graphene-reinforced iPP (G/iPP+CF) or graphene-modified reinforced iPP (G-PP/iPP+CF).
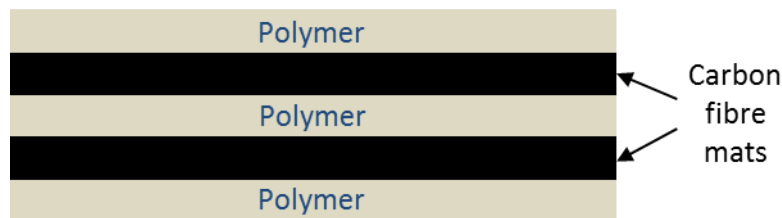
Figure 1. Schematic example of a laminate of iPP and carbon fibre mats.

Small portions of the laminates were cut to characterize the nanoindentation mechanical properties and the morphology by means of SEM. The samples were hold vertically in a plastic clip and embedded in epoxy resin. The cured mould was polished (Buehler, USA) with silicon carbide papers at decreasing grit size and using water as lubricant. Finally, the surface was polished with a microcloth disk soaked in a 0.3 μm alumina solution.

2.2. Methods

Embedded samples were measured in a G200 Nanoindenter (Keysight Tech., USA) using a continuous stiffness measurement (CSM) technique [4,5] and a low resolution head called dynamic contact module (DCM). A Berkovich tip with radius smaller than 20 nm was used. Standard fused silica was tested to perform the calibration of the tip area following the procedure described in [4]. During the loading cycle, a constant strain rate of 0.05 s^{-1} was applied and a small oscillation force of 1 nm of amplitude at a frequency of 75 Hz was superimposed. Storage modulus, E', and hardness, H, were determined through the continuous calculation of contact stiffness from the phase lag between oscillation force and harmonic displacement. The Oliver and Pharr method [4] was used considering

P. Enrique-Jimenez, S. Quiles-Díaz, H.J. Salavagione, M.A. Gómez-Fatou, F. Ania and A. Flores

elastic-viscoelastic performance [7]. A Poisson's ratio of 0.36 was assumed for the whole composite. SEM images were obtained, without metal coating, in a SU8000 Hitachi equipment.

3. Results and Discussion

The mechanical properties of all laminates were characterized in the vicinity of one CF and also far away from any fibre. For each laminate, mechanical maps (E' and H) around one isolated carbon fibre were obtained using an array of 25 x 25 indentations of $h = 50$ nm covering a region of 12.5 x 12.5 μm^2.

Fig. 2a shows the optical image of the region selected for the nanomechanical mapping on the iPP+CF sample (polymer layer without graphene). Fig. 2b illustrates the plot of E' as a function of h for selected indentations at three typical locations in the sample. A colour code has been used to distinguish each E' behaviour and the respective indent locations in Figure 2a. The green and red lines are associated to indentations produced on the polymer matrix and the CF, respectively, and both show a fairly constant E' value with penetration depth once E' is stabilized. In contrast, for the indentation initiated close to the CF edge (blue line), E' conspicuously rises when the indenter comes into contact with the fibre ($h \approx 35$ nm).
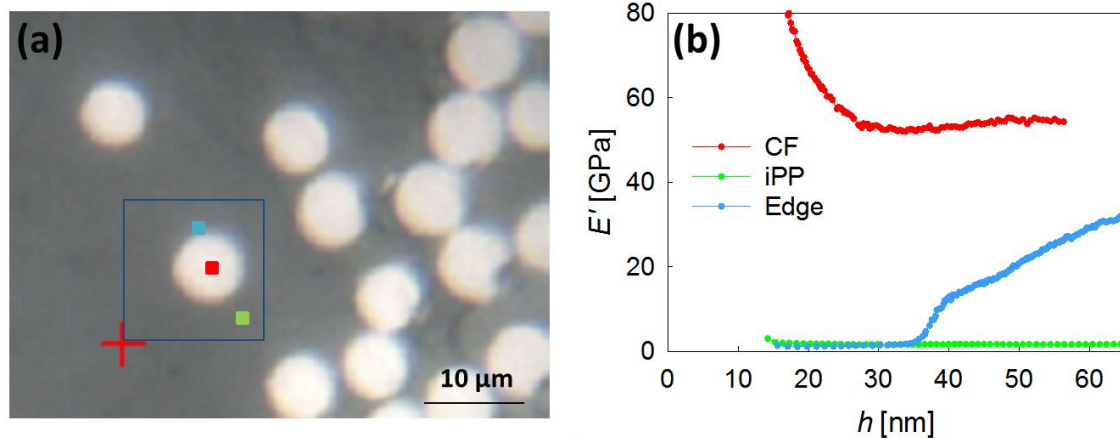
Figure 2. a. Optical image of the selected region for nanoindentation measurements on iPP+CF. The blue box denotes the array of 25 x 25 indentations separated by 0.5 µm. b. Plot of E' as a function of h for three indentations identified on Fig. 2a by a colour code.

Figure 3 shows the variation of E' along a number of scan lines that start at locations far away from the fibre, run across the matrix-fibre interface and ends up deep into the CF. Similar results were obtained for H and are not shown here for the sake of simplicity. The semi-logarithmic plot shows E' as a function of the distance between the point of initial contact and the edge of the CF (for $h = 50$ nm). Data for $E' < 4$ GPa appear to correspond to the polymer matrix and it seems that there is a slight rise of E' values as the fibre surface is approached (at ≈ 3.5 µm), i.e., immediately before the conspicuous rise of mechanical property associated to the CF contact. Results suggest that an interphase with distinct mechanical properties takes place at the boundary between the fibre and the matrix and a counting analysis was carried out to overcome the data scatter and better identify the mechanical properties of this transition region.

P. Enrique-Jimenez, S. Quiles-Díaz, H.J. Salavagione, M.A. Gómez-Fatou, F. Ania and A. Flores
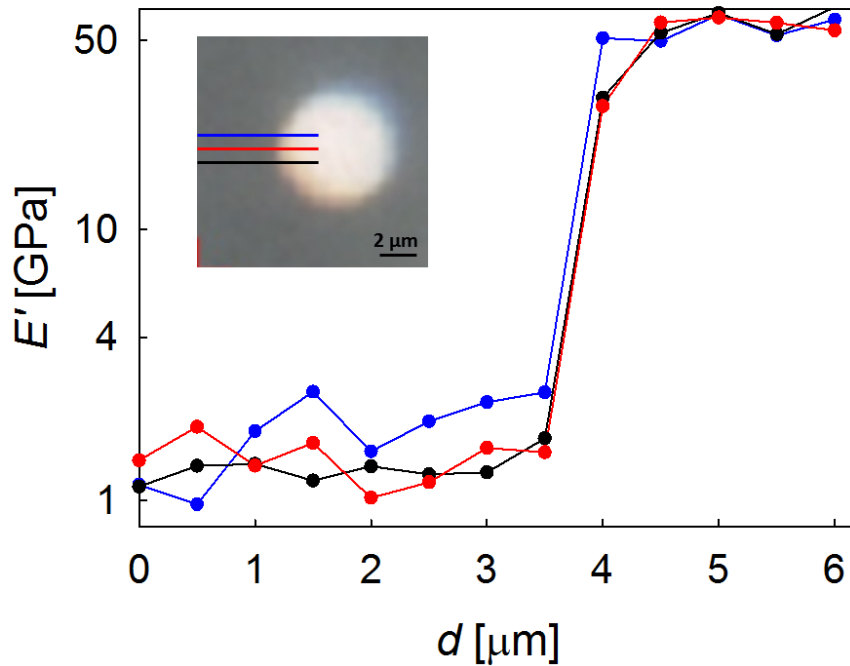
Figure 3. Variation of *E'* (*h* = 50 nm) as a function of the distance between the point of initial contact and the CF edge. Data follow the lines depicted in the inset (same colour code for lines and symbols).

Fig. 4 collects the results obtained from the counting analysis carried out on the mechanical map around one CF in the iPP+CF material (blue box of Figure 2a) (solid bars). A similar analysis has been carried out far away from any CF (pattern bars). It is found that the *E'* maximum of both distributions is located around 1-2 GPa and the *E'* values above 5 GPa are related with the CF. Most interesting, data between 2 and 3.5 GPa are only found in the vicinity of the CF, suggesting the appearance of an interphase a few micrometers in size.
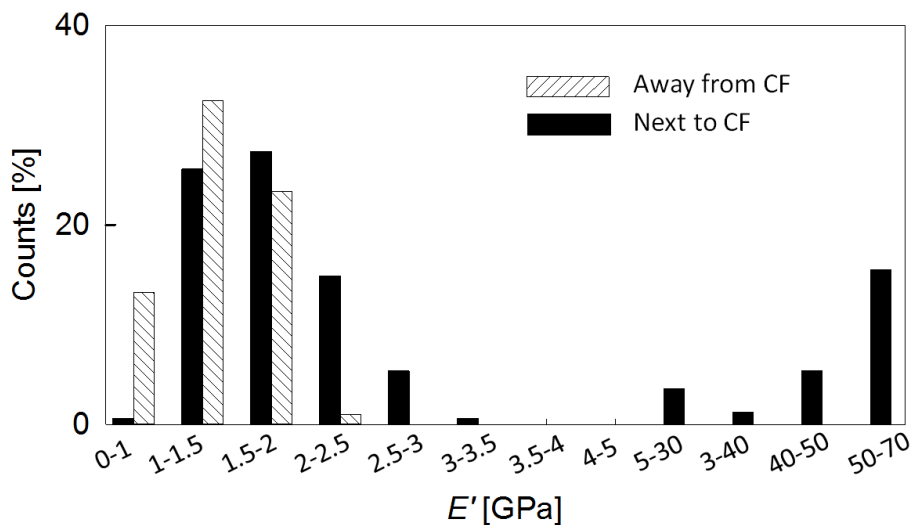
Figure 4. Frequency of appearance of each *E'* interval, for iPP+CF close to one CF (solid bars) and far away from any CF (pattern bars).

P. Enrique-Jimenez, S. Quiles-Díaz, H.J. Salavagione, M.A. Gómez-Fatou, F. Ania and A. Flores

A similar analysis was performed on the rest of laminates, where graphene has been incorporated to the polymer layer: one of them with modified graphene (G-PP/iPP+CF) and another one with non-modified filler (G/iPP+CF).

Fig. 5 shows the mechanical maps obtained using equivalent areas for all the laminates and the respective E' distributions after the data counting. The following colour code has been used for the mechanical maps: Indentations performed on the polymer matrix have been identified with green tones ($E' < 5$ GPa); red tones have been devoted to locations at the CF ($E' > 30$ GPa); blue tones correspond to tests starting on the polymer matrix and touching the CF at some stage. At first sight, it is found that the incorporation of graphene (Fig. 5b) produces a larger number of darker green spots (associated with higher E' values) as a consequence of the reinforcing effect of the filler. It is also remarkable that the mechanical enhancement for the case of modified graphene is significantly more limited (Figure 5c). This result suggests that the "soft" polymer brushes attached to the surface of graphene significantly contribute to the indentation behaviour.
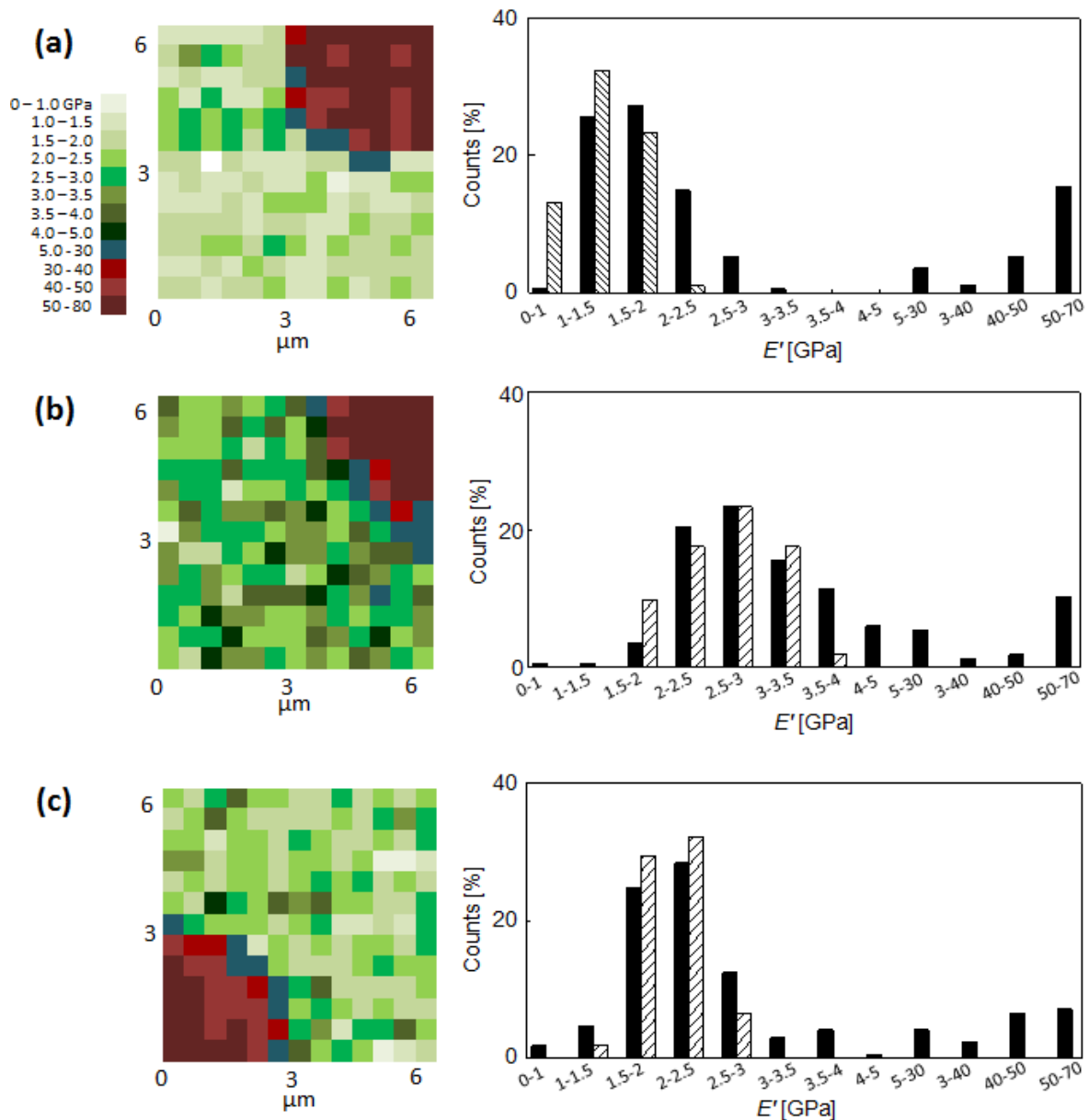
Figure 5. On the left, mechanical maps on selected regions of (a) iPP+CF, (b) G/iPP+CF and (c) G-PP/iPP+CF. The colour code for all maps is indicated at the top of the Figure. On the right, E'

P. Enrique-Jimenez, S. Quiles-Díaz, H.J. Salavagione, M.A. Gómez-Fatou, F. Ania and A. Flores

distributions after counting of the data on the left (solid bars) and for data far away from any CF (patterns bars).

Comparison of the E' distributions far away from any CF (pattern bars) for the three laminates clearly shows a shift of the whole distribution to higher values upon incorporation of the filler, especially in the case of neat graphene. In the case of G/iPP+CF, comparison of the distributions close and far away from the CF reveals that a significant number of data in the range $E' = 3.5 - 5$ GPa appear in the former case. It is noteworthy that this interval is marginal for iPP+CF and decreases in importance for G-PP/iPP+CF and would be in agreement with the accumulation of graphene at the CF front. Indeed, Fig. 6 shows SEM images including the regions selected for mechanical mapping (marked by blue squares). The appearance of darker green spots on the maps of Figs. 5b and 5c does not seem to match precisely with the locations of graphene layers on the SEM images (Figs. 6b and 6c). This discrepancy could be explained on the basis of the different operation mode of SEM and nanoindentation: while typical e-beam penetrations are of only a few nm, the deformation volume on nanoindentation experiments could be approximated to a hemisphere of radius in the range of hundreds of nm. Nevertheless, Figs. 6b and 6c show that some accumulation of graphene takes place at the fiber-matrix boundary. Indeed, Fig. 6d shows the CF front at a lower magnification in the G/iPP+CF sample. This image suggests that CFs act as a barrier to graphene and that the filtration of graphene throughout the CF mat is limited.
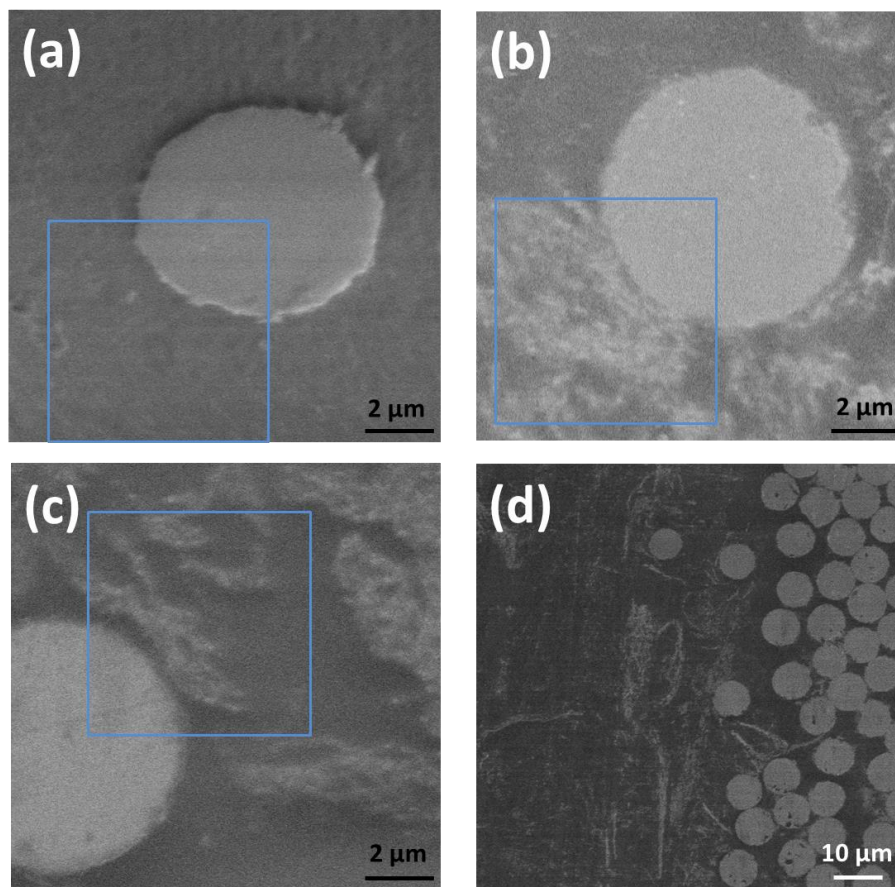
Figure 6. SEM images of the regions selected for the nanoindentation studies shown in Fig. 5 (identified by blue squares): (a) iPP+CF, (b) G/iPP+CF and (c) G-PP/iPP+CF. (d) Lower magnification of the fiber-matrix boundary in the G/iPP+CF material.

P. Enrique-Jimenez, S. Quiles-Díaz, H.J. Salavagione, M.A. Gómez-Fatou, F. Ania and A. Flores

4. Conclusions

It has been shown that nanoindentation can distinguish between the polymer matrix, the carbon fibres and the matrix-fibre interface in multilaminar iPP/CF laminates. Reinforcement of the polymer by the incorporation of graphene clearly produces a mechanical enhancement that is homogeneously distributed throughout the entire iPP layer. Mechanical mappings have been carried out close and far away to one CF on each laminate, using indentations as small as 50 nm on grids of 25×25 indentations covering areas of 12.5 x 12.5 μm^2. The data counting analysis suggests: i) prior to the incorporation of graphene in the polymer layer, there is a range of E' values that seems to be associated to the occurrence of an interphase a few micrometers in size; ii) upon incorporation of the nanofiller, there is a clear shift of the entire E'-values distribution towards larger values; a result that is more significant in the case of neat graphene than in the modified one; iii) there is an enhanced transition region from the matrix to the fibre for the G/iPP+CF material, partly due to the accumulation of graphene at the CF front.

The work highlights the relevance of the study of the mechanical properties at a local scale to understand the consequences of nanofiller dispersion and microfiller-polymer interfaces and interphases on the final material performance.

References

[1] K. Hu, D.D. Kulkarni, I. Choi and V.V. Tsukruk. Graphene-polymer nanocomposites for structural and functional applications. *Progress in Polymer Science,* 39:1934–1972, 2014.

[2] A.M. Díez-Pascual, M.A. Gómez-Fatou, F. Ania and A. Flores. Nanoindentation Assessment of the Interphase in Carbon Nanotube-based Hierarchical Composites. *Journal of Physical Chemistry C,* 116:24193–24200, 2012.

[3] A.M. Díez-Pascual, M.A. Gómez-Fatou, F. Ania and A. Flores. Nanoindentation in polymer nanocomposites. *Progress in Material Science*, 67:1-94, 2015.

[4] W.C. Oliver and G.M. Pharr. An improved technique for determining hardness and elastic-modulus using load and displacement sensing indentation experiments. *Journal of Material Research*, 7:1564-1586, 1992.

[5] J.B. Pethica and W.C. Oliver. Mechanical properties of nanometer volumes of material: use of the elastic response of small area indentations, in: J.C. Bravman, W.D. Nix, D.M. Barnett and D.A. Smith (Eds.). Thin films: Stresses and mechanical properties. *Materials Research Society Symposia Preceeding,* vol. 130:13. *Materials Research Society, Pittsburgh, USA*, 1989.

[6] S. Quiles-Díaz, P. Enrique-Jimenez, D.G. Papageorgiou, F. Ania, A. Flores, I.A. Kinloch, M.A. Gómez-Fatou, R.J. Young and H.J. Salavagione. Influence of the chemical functionalization of graphene on the properties of polypropylene-based nanocomposites. *Composites: Part A,* 100:31-39, 2017.

[7] E.G. Herbert, W.C. Oliver and G.M. Pharr. Nanoindentation and the dynamic characterization of viscoelastic solids. *Journal of Physics D: Applied Physics*, 41:74021, 2008.